



ELSEVIER

Available online at www.sciencedirect.com

Procedia Engineering 2 (2010) 603–612

**Procedia
Engineering**

www.elsevier.com/locate/procedia

Fatigue 2010

Fatigue assessment of naval welded assemblies

Carole Erny^{a,b*}, David Thevenet^a, Jean-Yves Cognard^a, Manuel Körner^b^aLaboratoire Brestois de Mécanique et des Systèmes,

ENSIETA, 2 rue François Verny, 29806 Brest Cedex 9, France

^bDCNS Ingénierie Navires Armés, rue Choiseul, 56311 Lorient Cedex, France

Received 5 March; revised 11 March; accepted 15 March

Abstract

Ship structures are commonly assembled by using welding process and they are submitted to some variable and complex loadings. Moreover, near the weld toe, some local stress concentrations are generated. Accordingly, welded joints could be a critical area regarding fatigue damage. In a previous work, a methodology to predict fatigue life has been developed and tested on butt-welded joints. The present work focuses on more complex assemblies in order to be able to estimate the fatigue life of representative naval structures. The strategy could be split into two steps. First, finite element calculation is performed with constant or variable amplitude loadings in order to analyze the elastic shakedown of the structure. To characterize the material heterogeneity of the welded joint, experimental tests on simulated heat affected zone and some micro-hardness measurements have been conducted. If the structure shakedown, a post-treatment has been developed to predict the fatigue crack initiation which is based on a two-scale damage model initially developed by Lemaitre et al., using again the heterogeneity of fatigue material properties, in order to obtain an accurate numerical predicted fatigue life. To validate this methodology, some experimental tests have been performed on various welded structures (cruciform joints type representative of naval assemblies) and comparisons between experimental and numerical fatigue life are encouraging.

© 2010 Published by Elsevier Ltd. Open access under [CC BY-NC-ND license](http://creativecommons.org/licenses/by-nc-nd/3.0/).*Keywords:* fatigue crack initiation; welded joint; two-scale model; stiffened panel

1. Introduction

Ship assemblies are usually built by using welding processes. This process induces variations of geometry near the weld toe which create local stress concentrations. Moreover, the heating and the subsequent cooling modify the material mechanical properties in this specific area. Due to the swell, these assemblies are submitted to cyclic variable loadings. Thus, welded joints are critical areas regarding fatigue damage and experimental observations point out that fatigue cracks initiate in the weld toe. Many authors [1-4] have already developed different models to estimate fatigue life span. But in most cases, the characteristic of the welded joint like weld toe geometry, the material heterogeneity or the residual stresses, are not taken into account. In a previous study [5], a strategy, considering several welded specificities, has been developed to predict fatigue life span and applied on butt-welded

* Corresponding author. Tel.: +332-98-34-88-07; fax: +332-89-34-87-30.

E-mail address: carole.erny@ensieta.fr

and cruciform joints. Some good correlations have been observed between experimental and numerical fatigue life span. So, the aim of the current work is to apply this strategy to more complex structures representative of naval assemblies such as stiffened panels.

The proposed methodology, developed for welded assemblies, contains two stages: the structure shakedown study and the fatigue crack initiation study. Finite element analysis (FEA) is used to determine the cyclic behavior of the structure which is submitted to constant or variable amplitude loadings. This calculation takes into account the cyclic behavior of constitutive materials of the joint: base metal (BM), heat affected zone (HAZ) and melt metal (MM). Micro-hardness measurements have been carried out on welded profiles to better characterize the mechanical behavior of the different materials and the so called interface between the different regions. Thanks to these measurements, the heterogeneity of mechanical properties can be taken into account in the calculation. To have a better description of the weld, monotonic and cyclic tests have been carried out on the base metal and on a simulated HAZ. Moreover, some laser measurements have also been carried out to well model the geometry of the weld toe.

If the structure shakedown i.e. the behavior becomes elastic after a quite low cycles, a post-treatment can predict the period needed to initiate a fatigue crack. This calculation is based on a two-scale damage model initially developed by Lemaitre et al. [6]. In this stage, the main specificities of the weld are also taken into account by linking the material parameters of the model to the micro-hardness. To evaluate the accuracy of the proposed strategy, some tests have been carried out and a comparison between experimental and numerical results is established for stiffened panels.

Nomenclature

ρ, θ	weld toe radius, weld toe angle
R	stress ratio
H_v	Vickers hardness
$\sigma_{a \text{ nom}}$	nominal stress (amplitude)
σ_f	fatigue limit (amplitude)
σ_u	ultimate strength
ν	Poisson's ratio
E	Young's modulus
h	micro-default closure parameter
D_c, D_{1c}	critical damage, critical damage (monotonic uni-axial tension)
m	non-linear exponent
S, s	damage strength, damage exponent
p_D, ε_{pD}	damage threshold, damage threshold (monotonic uni-axial tension)
p	accumulated plastic strain
C, $C_1, C_2, \gamma_1, \psi, \varphi_\infty$	kinematic hardening parameters
b, Q, R_1	isotropic hardening parameters
X, X_1, X_2	kinematic hardening tensors
$\varepsilon^e, \varepsilon^p, \varepsilon$	elastic, plastic and total strain tensor in the inclusion
ε^m, σ	strain tensor, stress tensor in the matrix

2. Sample description

2.1. Welded joint

This work focuses on welded assemblies typical of shipbuilding applications. The chosen structure is a transversal and longitudinal stiffened panel commonly used for the framework of the ship (Figure 1). A semi-automatic MAG (Metal Active Gas) process was used to weld all panels together (Figure 1). Each panel has a specific thickness respectively of 8 mm for the main plate, 6.2 mm for the transversal stiffener (floor) and 5 mm for the longitudinal stiffener (holland profile). The width of the assembly is about 130 mm and the effective section area

is about 1412 mm². Moreover, in order to reduce the influence of residual stresses, welded specimens were systematically submitted to a stress relieving by heat treatment at 600°C for 30 minutes.

The geometry of the weld toe is evaluated by laser measurement. This technique provides the toe radius and the toe angle. One sample was scanned and the minimum value obtained is about 0.5 mm (Figure 1). This value is used to model a welded configuration in the FEA. Depending on the tested sample, different geometries can be observed and be more or less severe. A smaller weld toe radius, for example, increases the stress concentration at the weld toe and provides a more critical area regarding to fatigue damage.

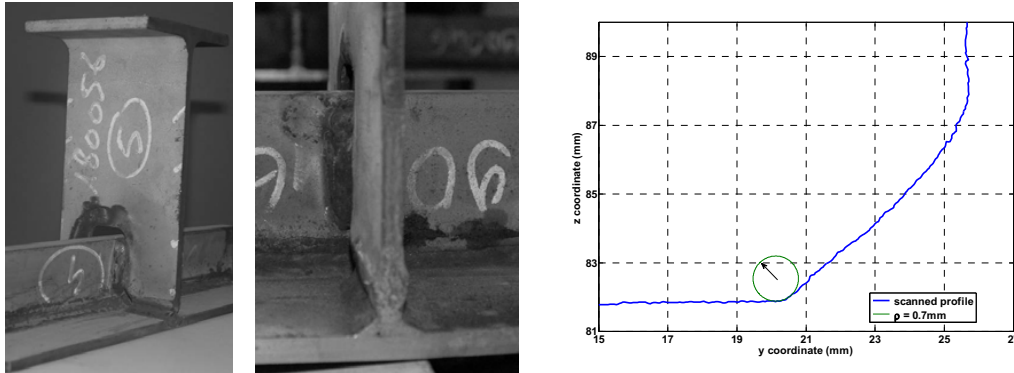


Figure 1: (a) Picture of the studied welded assembly (effective zone), (b) Zoom between the bottom plate and the floor, (c) Scanned profile

2.2. Materials description and characterization

The aim of this study is to validate a numerical method to estimate fatigue life of welded structures. The FEA and the post-treatment require a set of materials parameters to take into account the mechanical behaviors. All samples used in this part were prepared with DH36 steel. Experimental tests are needed to determine these parameters. Thus, monotonic, cyclic and self-heating tests [7] tests have been performed on a servo-hydraulic fatigue testing machine with a capacity of ± 100 kN. Tests were conducted using cylindrical specimens with a diameter of 8 mm and effective length of 12 mm. Tests were carried out for two different stress ratios: $R = 0.1$ and $R = -1$.

The self-heating test provides a fast estimation of high cycle fatigue properties: S-N curve and fatigue limit. It consists in applying successive series of cycles with different increasing stress amplitudes; at each step, the change of the temperature variation is measured and a significant increase is observed close to the fatigue limit. Thanks to this fatigue limit and fatigue life obtained for the last stress amplitude, the experimental S-N curve is obtained by using the Stromeier's law.

In order to take into account the heterogeneity of the weld, all the previous tests were also performed on a simulated HAZ (DH36/HAZ). To obtain this simulated HAZ, a DH36 plate was heat treated at 1,000°C for 24 minutes and then it was cooled in oil. Unfortunately, the melt metal has not been characterized due to the difficulties to obtain specimens.

Experimental cyclic curves point out a variation of the yield strength between the monotonic and the cyclic behaviors. Thus, the elastic-plastic model developed by Lemaitre and Chaboche [8-9] has been used to describe the materials behavior. This model uses a combination of one isotropic hardening and two kinematic hardenings. Moreover, DH36/HAZ cyclic curves point out a softening; thus in order to describe this behavior, the kinematic hardening model developed by Marquis [10] is used. The elasticity is described by a Hooke's law:

$$\epsilon^e = \frac{1+\nu}{E} \sigma - \frac{\nu}{E} (Tr \sigma) I \quad (1)$$

The elastic domain is described by the yield criterion ($f \leq 0$):

$$f = J_2(\sigma - X_1 - X_2) - R - \sigma_y \leq 0 \tag{2}$$

The isotropic hardening is needed to allow the variation between the monotonic and the cyclic yield strength and its evolution law is defined by (3) and the kinematic evolution laws are defined by (4):

$$\dot{R}_1 = b (Q - R_1) \dot{p} \tag{3}$$

$$\dot{X}_1 = \frac{2}{3} C_1 \dot{\epsilon}_p - \gamma_1 \dot{X}_1 \dot{p} \text{ and } \dot{X}_2 = \frac{2}{3} C_2 \dot{\epsilon}_p - \gamma_2(p) \dot{X}_2 \dot{p} \text{ with } \gamma_2(p) = \varphi_\infty + \psi e^{-\omega p} \tag{4}$$

All these experimental tests provide a set of parameters for each metal (Table 1) which well describe their behavior (Figure 2). Some micro-indentations carried out on a weld profile indicate that there is a variation of the micro-hardness through the joint. Thus, the monotonic and cyclic curves allow identifying the hardening parameters of two areas of the joint where the micro-hardness is well-known: $H_v = 200$ for the base metal and $H_v = 275$ for the simulated HAZ. In this way, a linear law has been established to link the hardening parameters to the micro-hardness. Thereby, the monotonic and cyclic behaviors of any part on the joint can be described by the only knowledge of its micro-hardness (Figure 3).

Table 1: Parameters of the elastic-plastic model

DH36	σ_y (MPa)	b	Q (MPa)	C_1 (MPa)	γ_1	C_2 (MPa)	ω	φ_∞	ψ
BM	300	89	-50	4260	15.6	38300	10	252	106
HAZ	400	15	-100	8890	27.7	101300	10	418	19

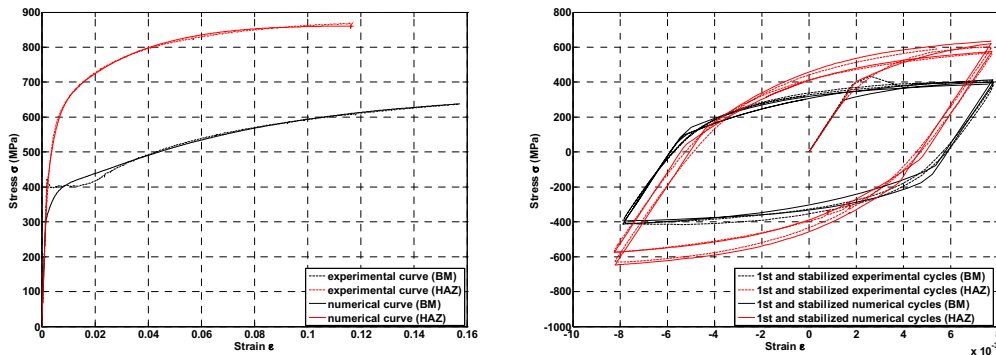


Figure 2: (a) Experimental and model response for BM and HAZ: monotonic tensile test, (b) Cyclic tension-compression test

The validation of the hypothesis that a linear law links the hardening parameters to the micro-hardness is actually under consideration. The micro-hardness measurements are performed using an instrumented Vickers micro-indenter which provides the load-displacement curve of the indenter during the test. Based on these data, the micro-hardness is obtained by using the Oliver and Pharr method [11]. Through the weld profile, the micro-hardness could easily be determined. Our aim is to numerically model a micro-indentation test with specific hardening parameters and to compare this response to the experimental load-displacement curve. The first comparisons performed for BM are encouraging and other indentation calculations with intermediate parameters are under achievement.

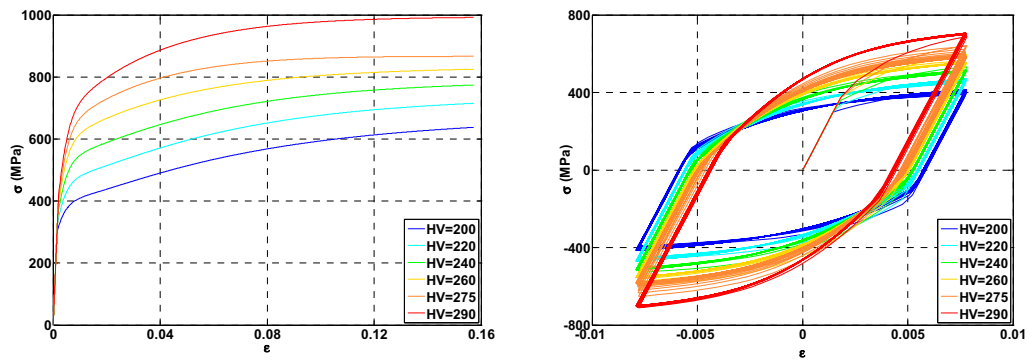


Figure 3: Evolution of the monotonic and cyclic behaviors with micro-hardness

2.3. Post-treatment: a two-scale damage model

The main aim of the present work is to study the high cycle fatigue life of representative shipbuilding welded assemblies. In this domain, the macroscopic behavior of the structure is elastic that is why only the loading cases inducing an elastic shakedown are taken under consideration. The fatigue damage is due to micro-plasticity so it seems fair to use a two-scale damage model to estimate the fatigue life span. The two-scale damage model initially developed by Lemaitre et al. [12] has been chosen. In this model, the elastic shakedown state is used at a macroscopic scale and the damaging elastic-plastic behavior is used at a microscopic scale. A representative volume element (RVE) made of an elastic matrix with an elastic-plastic inclusion which can suffer damage is considered. The inclusion of the RVE is a mechanical inclusion without physical size. The fatigue damage occurs due to the micro-plasticity and then the yield strength of the inclusion is taken equal to the fatigue limit. As a result, fatigue crack can only initiate if the local loading is higher than this limit. Over the elastic domain, fatigue damage occurs. When this damage reaches a critical value, a crack appears in the inclusion and we consider that there is fatigue crack initiation in the RVE. The elastic-plastic strains in the inclusion ϵ are linked to the elastic strains in the matrix ϵ^m by a localization law:

$$\epsilon - \beta \epsilon^p = \epsilon^e + (1 - \beta) \epsilon^p = \epsilon^m \text{ with } \beta = \frac{2(4 - 5\nu)}{15(1 - \nu)} \tag{5}$$

where ϵ^e et ϵ^p are, respectively, the elastic and the plastic strain in the inclusion, β is given by the Eshelby [13] analysis of a spherical inclusion and ν is the Poisson's ratio. Coupling between elastic strain and isotropic damage D is based on the concept of effective stress $\tilde{\sigma}$, what conduces to the following elastic law :

$$\epsilon^e = \frac{1 + \nu}{E} \tilde{\sigma} - \frac{\nu}{E} (Tr \tilde{\sigma}) I = \frac{1 + \nu}{E} \frac{\sigma}{1 - D} - \frac{\nu}{E} \left(Tr \frac{\sigma}{1 - D} \right) I \tag{6}$$

where σ is the stress tensor, E is the Young's Modulus and I the second-order identity tensor. Inclusion's yield strength is the fatigue limit σ_f . Considering a linear kinematic hardening X and the von Mises criterion J_2 , the yield function $f = 0$ is written as:

$$f = J_2(\tilde{\sigma} - X) - \sigma_f \tag{7}$$

Plastic strains, linear kinematic hardening and damage evolutions laws are:

$$\dot{\varepsilon}^p = \frac{3}{2} \frac{\tilde{\sigma}^d - X}{J_2(\tilde{\sigma} - X)} \dot{p} \quad \text{with} \quad \tilde{\sigma}^d = \tilde{\sigma} - \frac{1}{3} \text{Tr} \tilde{\sigma} \mathbf{I} \quad (8)$$

$$\dot{X} = \frac{2}{3} C (1-D) \dot{\varepsilon}^p \quad \text{with} \quad \dot{D} = \left(\frac{Y}{S} \right)^s \dot{p} \quad (9)$$

where the damage strength S and the damage parameter s are material parameters, p is the accumulated plastic strain, p_D is the damage threshold and Y is the strain elasticity energy density release rate defined by:

$$Y = \frac{1+\nu}{2E} \left[\frac{\text{Tr}(\langle \sigma \rangle_+^2)}{(1-D)^2} + h \frac{\text{Tr}(\langle \sigma \rangle_-^2)}{(1-hD)^2} \right] - \frac{\nu}{2E} \left[\frac{\langle \text{Tr} \sigma \rangle_+^2}{(1-D)^2} - h \frac{\langle -\text{Tr} \sigma \rangle_-^2}{(1-hD)^2} \right] \quad (10)$$

where $\langle \cdot \rangle_+$ means the scalar positive part (i.e. $\langle x \rangle_+ = x$ if $x \geq 0$ and $\langle x \rangle_+ = 0$ if $x < 0$), h is a micro-default closure effect parameter. When damage D reached its critical value D_c , it corresponds to a crack initiation at mesoscopic scale. This critical damage depends on loading and is linked to critical damage under monotonic uni-axial tension D_{lc} and the ultimate strength σ_u :

$$D_c = D_{lc} \frac{(\sigma_u)^2}{2EY} \quad (11)$$

A right indicator for prediction of damage initiation is the stored energy. We suggest calculating this energy at the end of each cycle with the higher stress value $\sigma_{eq} = cste = \sigma_{eq}^{max}$ considering there is a perfect plasticity. The damage threshold p_D may be written as a function of ultimate strength σ_u , fatigue limit σ_f , damage threshold under monotonic uni-axial ε_{pD} and a non-linearity exponent m :

$$p_D = \varepsilon_{pD} \left[\frac{\sigma_u - \sigma_f}{\sigma_{eq}^{max} - \sigma_f} \right]^m \quad (12)$$

All parameters of this model are identified following a process defined in a previous work [14] in which only one monotonic curve and two S-N curves are needed. The identification has only been carried out for both metals (Figure 4) and a linear law has been established between fatigue parameters and micro-hardness and finally, only three parameters (s , σ_f , σ_u) depend on micro-hardness measurements. The proposed model can describe an S-N curve for any micro-hardness and any stress ratio (Figure 4). The obtained parameters identified for BM and HAZ are summarized in Table 2.

Table 2: Parameters of the two-scale damage model

DH36	C (MPa)	E (GPa)	ν	σ_u (MPa)	D_{lc}	h	ε_{pD}	m	S (MPa)	s	σ_f (MPa)
BM	2 500	210	0.3	630	0.3	0.2	0.02	1.85	200	0.53	180
HAZ	2 500	210	0.3	870	0.3	0.2	0.02	1.85	200	0.84	230

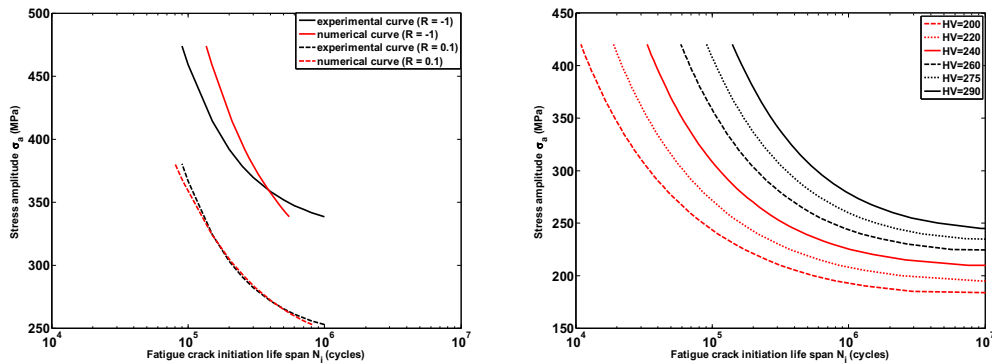


Figure 4: (a) Experimental S-N curves and fatigue model response for HAZ, (b) variation of fatigue properties with $R = -0.2$

3. Fatigue tests

Welded assemblies have been tested on a multi-axial fatigue machine using a ± 400 kN hydraulic actuator in laboratory air at room temperature. Due to the dissymmetry of the assembly, they are not submitted to compressive loads to avoid buckling and to be sure to keep the same loading axis. So, tests have been conducted with a positive stress ratio ($R = 0.1$).

A specific anchorage system has been designed to link the samples to the actuator and to the support. The first part of the system consists in three steel parts which grip the sample and an intermediate part which connects these three parts to the hydraulic actuator. On the opposite side, the sample is linked to the clamping bracket using an equivalent anchorage system (Figure 5).

The stop criterion is based on the ACPD (Alternating Current Potential Drop) signal [15]. This system allows detecting very small cracks by measuring the voltage variation in several areas of the sample. Indeed, if a crack appears, there is a local variation of electrical resistance and then, a voltage variation is observed. Generally, fatigue cracks appear near the surface: thus, a low intensity current (0.5 A) with high frequency (25 kHz) has been used. The geometry induced by the weld toe creates some stress concentrations, so the voltage measurements are only performed in these critical areas.

Fatigue tests have been conducted under load control. The load axis, in the longitudinal direction of the specimen, is applied at the center of gravity of the cross section. Moreover, some rosette strain gages have been used to ensure the strain state in the structure and thus, validate the applied tensile loading. The strain state is measured far from the welded joint to avoid effects of local stress concentrations.

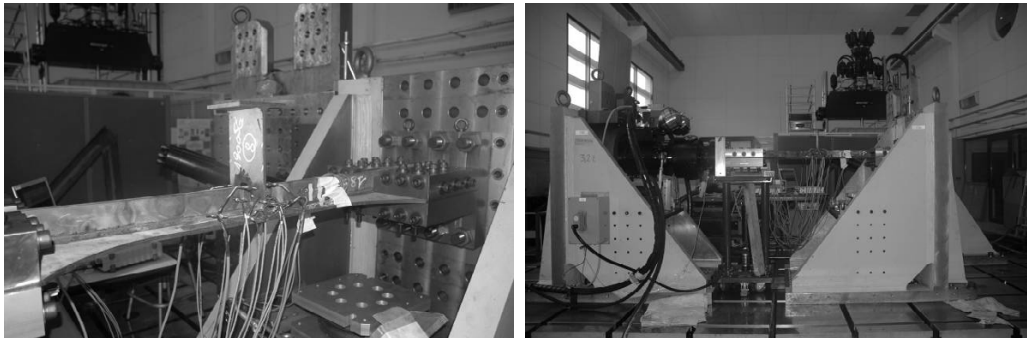


Figure 5: Anchorage system and ACPD equipment on the multi-axial fatigue machine

4. Fatigue life estimation

The first stage of the proposed strategy consists in FEA to determine the cyclic behavior of the structure and especially if an elastic shakedown can occur or not. Calculations have been performed with Abaqus software using 3D-element (C3D6 and C3D8). Due to the symmetry of the sample, only one half of the sample is modeled with two different geometries of the weld toe. For both configurations, the toe angle is equal to 45° and the effective throat thickness is equal to 4 mm. There is only a variation of the toe radius with is respectively equal to 0.5 and 0.7 mm. The first radius is the minimum value obtained from experimental measurements and the second is mean value. The weld beads are a particular point of interest so they were meshed with smaller elements: the element size is about 0.05 mm (Figure 6). The global model is meshed with about 1.6 million of elements. The welding process creates heterogeneity of mechanical properties through the joint. It has been noticed this variation can be link to the micro-hardness. Thus, the micro-hardness field is introduced in the calculation by using a user subroutine (UFIELD). Thanks to these data, the heterogeneity of mechanical properties is also taken into account. In fact, another user subroutine (UMAT) allows introducing evolution of the hardening parameters with the micro-hardness. So, at each point of the structure, a micro-hardness value is introduced which allows to define the monotonic and the cyclic material behaviors at this point (Figure 6). Since the load axis is the longitudinal direction of the specimen, nearly no stress concentration appears near the welded joint which links the main plate and the holland profile. In order to reduce calculation time, no micro-hardness variation is introduced along this welded joint. Calculations were performed under different nominal stress amplitude $\sigma_{a\ nom}$, from 80 MPa to 110 MPa, on both geometrical configurations ($\rho = 0.5\ mm$ and $\rho = 0.7\ mm$). But, only cases in which an elastic shakedown occurs are used in the post-treatment. Moreover, the first elastic-plastic calculations point out three critical areas, named weld 1 to weld 3, localized near the curvature of each welded joint (Figure 6).

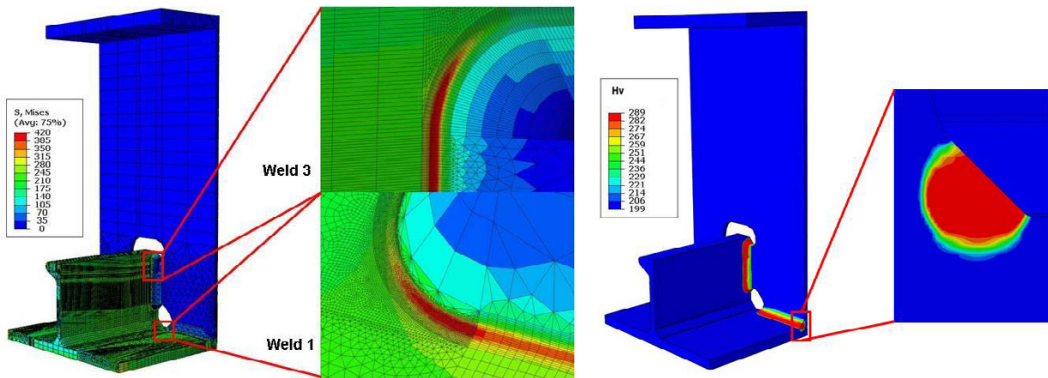


Figure 6: (a) Mesh and von Mises equivalent stress of a stiffened panel: $\sigma_{a\ nom} = 90\ MPa$, $R = 0.1$ and $\rho = 0.7\ mm$ (1/2 part of the effective zone), (b) Micro-hardness field of a stiffened panel (1/2 part of the effective zone)

In these specific zones, the stress tensor points out a multi-axial stress state mainly due to the floor. Due to the plasticity appearing in the first cycles, the local stress ratio can be different from the applied one. For instance, the maximum and the minimum stress tensors are (in MPa):

$$\sigma_{max} = \begin{pmatrix} 65 & 89 & 0 \\ 89 & 472 & -2 \\ 0 & -2 & 130 \end{pmatrix} \quad \sigma_{min} = \begin{pmatrix} 15 & -2 & 0 \\ -2 & 15 & 0 \\ 0 & 0 & 28 \end{pmatrix} \quad (13)$$

These values are located in weld 3, during the stabilized cycle (shakedown), submitted to a nominal stress amplitude $\sigma_{a\ nom} = 90\ MPa$ following the second direction, a stress ratio $R = 0.1$ and $\rho = 0.7\ mm$.

5. Results

The post-treatments, performed on two different configurations ($\rho = 0.5$ mm, $\rho = 0.7$ mm), point out that fatigue crack initiates at the welded joint which connects the two stiffeners (weld 3, Figure 6). Moreover, the stress state largely depends on the weld toe value introduced in the FEA: the results obtained with $\rho = 0.5$ mm always provide the shorter fatigue life (Figure 7). If the same value of ρ is introduced in the three zones, the first fatigue crack always initiates in weld 3. However, if several values of ρ are identified in these three areas, this fatigue crack can initiate in the two other joints (weld 1 or weld 2, Figure 7).

The proposed strategy is deterministic so the modeled geometry is not a realistic representation of the sample, it is just representative. Based on laser measurements, the chosen weld toe radius is taken as one which introduces the highest stress concentration. So, the calculation should always provide some safety results.

If the experimental toe radius of weld 1 or weld 2 is smaller than the toe radius of weld 3, the numerical and experimental fatigue crack initiation will not be localized at the same area. This effect appeared in the first tested sample and it was mainly due to a lack of continuity in the weld (geometrical defect). In this first test, nominal stress amplitude of 90 MPa with a stress ratio equal to 0.1 was applied. Experimentally, the fatigue crack initiates at weld 2 after 265,000 cycles; the numerical prediction obtained with the proposed model is: 239,000 cycles for $\rho = 0.5$ mm. Thus, an encouraging prediction is obtained for the first experimental result on a representative structure of shipbuilding applications.

In fact, after more accurate laser measurements, it has been noticed that weld 1 and weld 3 were performed with higher toe radius. The manufacturing process of the sample was corrected to assume a similar geometry between the joints. Future experimental results should only present fatigue crack on weld 3 and so, the experimental fatigue lives would easily be compared to numerical estimations.

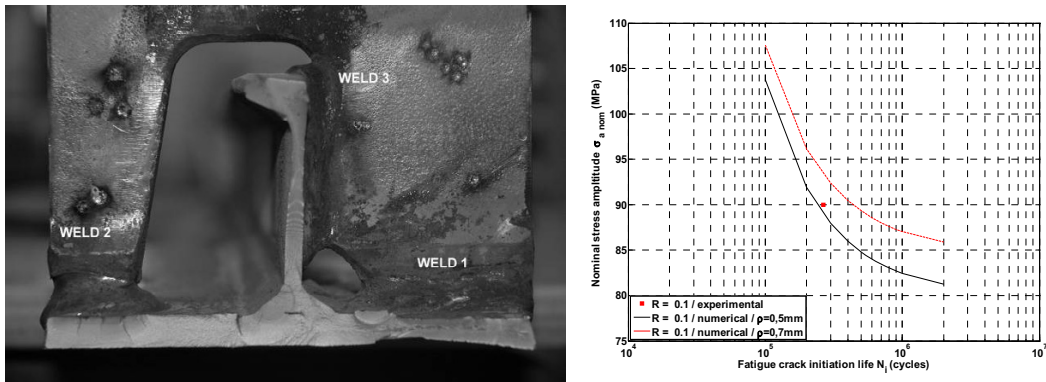


Figure 7: (a) Fracture surface with a first fatigue crack localized at the weld 2, (b) Numerical fatigue life of a stiffened panel ($\rho = 0.5$ mm and $\rho = 0.7$ mm) at the weld 3

6. Conclusion and prospects

In this study, a methodology to estimate fatigue life span is presented and a first application to representative stiffened panels typical of shipbuilding is proposed. The first stage consists of a finite element calculation to establish the elastic cyclic behavior of the structure under variable or constant amplitude loading. This calculation takes into account the heterogeneity of welded joint by using a micro-hardness field. A particular interest is made on the geometry of the welded toe to represent the stress concentration area. If an elastic shakedown occurs in the structure, a post-treatment is applied to determine the fatigue crack initiation life. This calculation is based on a two-scale damage model and takes also into account several specificities of a welded joint. To estimate the accuracy of the proposed strategy, experimental tests have been carried out on a fatigue machine using a 400 kN actuator. The

immediate prospect is to purchase tests in order to compare experimental and numerical results under several constant amplitude loads and different stress ratios and validate this approach dedicated to industrial applications.

Acknowledgements

The authors would like to thank DCNS group for financing this work and supplying welded specimens. The authors are grateful to P. Martinat and B. Mecucci from ENSIETA/DTN/CMA for their collaboration the manufacturing of grips and fixtures and S. Bourc'his and D. Penchenat from LBMS for their collaboration during the set-up of tests.

References

- [1] Radaj D., Sonsino C.M., Fricke W. *Fatigue assessment of welded joints by local approaches*, Woodhead publishing, Cambridge, CRC Press, 2nd edition, 2006.
- [2] Radaj D. Review of fatigue-strength assessment of non-welded and welded structures based on local parameters, *Int. J. Fat.*, 1996;**18**:153-70.
- [3] Hobbacher A, et al. Recommendations for fatigue design of welded joints and components. IIW doc. XIII-1965-03/XV-1127-03, 2006.
- [4] Taylor D., Barrett N., Lucano G. Some new methods for predicting fatigue in welded joints. *Int. J. Fat.*, 2002;**24**:509-18.
- [5] Lautrou N., Thevenet D., Cognard J.Y. Fatigue crack initiation life estimation in a steel welded joint by the use of a two-scale damage model. *Fat. Fract. Eng. Mat. Str.*, 2009, **32** (5), pp. 403-417.
- [6] Lemaitre J., Sermage J.P., Desmorat R. A two-scale damage concept applied to fatigue. *Int. J. Fract.*, 1999;**97**:67-81.
- [7] Doudard C., Calloch S., Hild F., Cugy P., Galtier A. A probabilistic two-scale model for high cycle fatigue life predictions. *Fat. Fract. Eng. Mat. Str.*, 2005;**28**:279-88.
- [8] Chaboche J. L.. Viscoplastic constitutive equations for the description of cyclic and anisotropic behavior of metals. *Bulletin Ac. Polonaise des Sciences, Série Sc. Et Techniques*, 1975;**25**:33-42.
- [9] Lemaitre J., Chaboche J. L. *Mechanics of solid materials*. Cambridge University Press, Cambridge, 1994.
- [10] Calloch S., Marquis D. Triaxial tension-compression tests for multiaxial cyclic plasticity, *Int. J. of Plast.*, 1999;**15**:521-49.
- [11] Oliver W.C., Pharr G.M. An improved technique for determining hardness and elastic modulus using load and displacement sensing indentation experiments. *Journal of Materials Research* 1992;**7**:1564-1583.
- [12] Lemaitre J., Desmorat R. *Engineering Damage Mechanics: Ductile, Creep, Fatigue and Brittle Failures*, Springer Verlag, Berlin, 2005.
- [13] Eshelby J.D. *Proc. Roy. Soc.* 1957;**A241**:376-96.
- [14] Emy C., Thevenet D., Cognard J.Y., Körner M. Experimental and numerical analyses of fatigue behavior of welded cruciform joints. *Journal of ASTM International*, uncorrected proof, 2010.
- [15] Matelect LTD. Practical aspects of the ACPD technique, User Manual.
- [16] Goodman J. *Mechanics applied to engineering*. Longmans, Green and Co., London, 1919, pp. 631-636.
- [17] Susmel L., Tovo R., Lazzarin P. The mean stress effect on the high-cycle fatigue strength from a multiaxial fatigue point of view. *Int. J. Fat.*, 2005;**27**:928-43.
- [18] Zhang Y.H., Stephen J. Maddox. Fatigue life prediction for toe ground welded joints. *Int. J. Fat.*, 2009;**31**:1124-36.
- [19] Radaj D. Fatigue notch factor of gaps in welded joint reconsidered. *Engng. Fract. Mech.*, 1997;**57**:14-148.
- [20] Lieurade H.P., Huther I., Lebaillif D. Weld quality assessment with regard to fatigue strength. *Méc. & Ind.*, 2005;**6**:133-43.